

QPO analysis of the TeV and X-ray lightcurve of Mkn 501 in 1997 - final results

D. Kranich¹, O. de Jager², M. Kestel¹, E. Lorenz¹, and For the hegra collaboration

¹MPI für Physik, München, Germany

²Potchefstroom University for CHE, Potchefstroom, South Africa

Abstract. The BL Lac object Mkn 501 was in a state of high activity in the X-ray and TeV range in 1997. Here we present the final results from a QPO analysis of the HEGRA and RXTE data. Evidence for a 23-day periodicity is supported at the 3.4 sigma level, depending on various model assumptions.

1 Introduction

The 1997 flare of Mkn 501 (Protheroe, 1997 for an overview) with its long duration and significant flux variations allowed for the first time to carry out a periodicity analysis in the TeV energy range. Since then, several groups reported about indications for a periodic structure (23 days) in the TeV lightcurve (Kranich, 1999 and reference therein). The 23 day period was also found in the 2-10 keV X-ray band observed by the all sky monitor (ASM) of RXTE.

The first results from the QPO-analysis of the HEGRA data has already been presented at the last ICRC (1999) in Salt Lake City (Kranich, 1999; de Jager, 1999). In this first analysis an attempt was made to take into account the flaring behavior of Mkn 501 in the probability calculation of the observed period. Nevertheless, some questions concerning the reliability of the analysis remained open. The main issues were:

- Does the exponential probability distribution of the renormalized Fourier power (Kranich, 1999, eq. 5), which was supported by the data, really hold?
- Is the used Lomb-Scargle (LS) periodogram, to derive the power spectra, suitable to estimate the parameters of the shot noise model?
- Is the combination of the results from the X-ray and TeV power spectra valid, i.e., are the two power spectra independent?

These issues are addressed in this paper.

Correspondence to: D. Kranich (daniel@mppmu.mpg.de)

2 The data

The TeV data were taken with the 6 Cherenkov telescopes of the HEGRA collaboration. 110 hours of observation were taken with the CT stereo-system and about 300 hours with the two telescopes CT1 and CT2. A sizable fraction of the CT1 data was taken during moonshine, thus providing measurements when no other telescope was operational (Kranich, 1999b). The CT1 data has been completely reanalyzed since (Kranich, 1999) and the moon observation data has been improved (Kranich 2001). The same time range as previously (MJD 50545 - 50661) has been used for the QPO analysis. The TeV and X-ray lightcurves are shown in fig. 1.

The x-ray data were recorded with the ASM on board the RXTE satellite in the 2 to 10 keV band (Remillard, 1997). They are available on the RXTE/ASM web page.

3 Probability distribution of the Fourier power

The *shot noise model* denotes the response of a linear system to input data which consists of a large number of randomly distributed shots with random amplitude. In the case of AGN, shots are identified with the interaction of a shock wave with a plasma 'blob'. The system response function which reveals itself in the shape of the individual flares is given by the γ -production model.

The mean Fourier power spectrum of the shot noise model has a characteristic shape which mainly depends on the system response function. Once the shape is known, it is possible to calculate the probability of a peak in the Fourier power spectrum of a given source. This probability is then given against the null hypothesis of randomly distributed flares of a certain shape. This is shown in the following.

The input data $x(t)$ of the shot noise model is given by the following Ansatz:

$$x(t) = \sum_{i=1}^K a_i \cdot \delta(t - \tau_i) \quad (1)$$

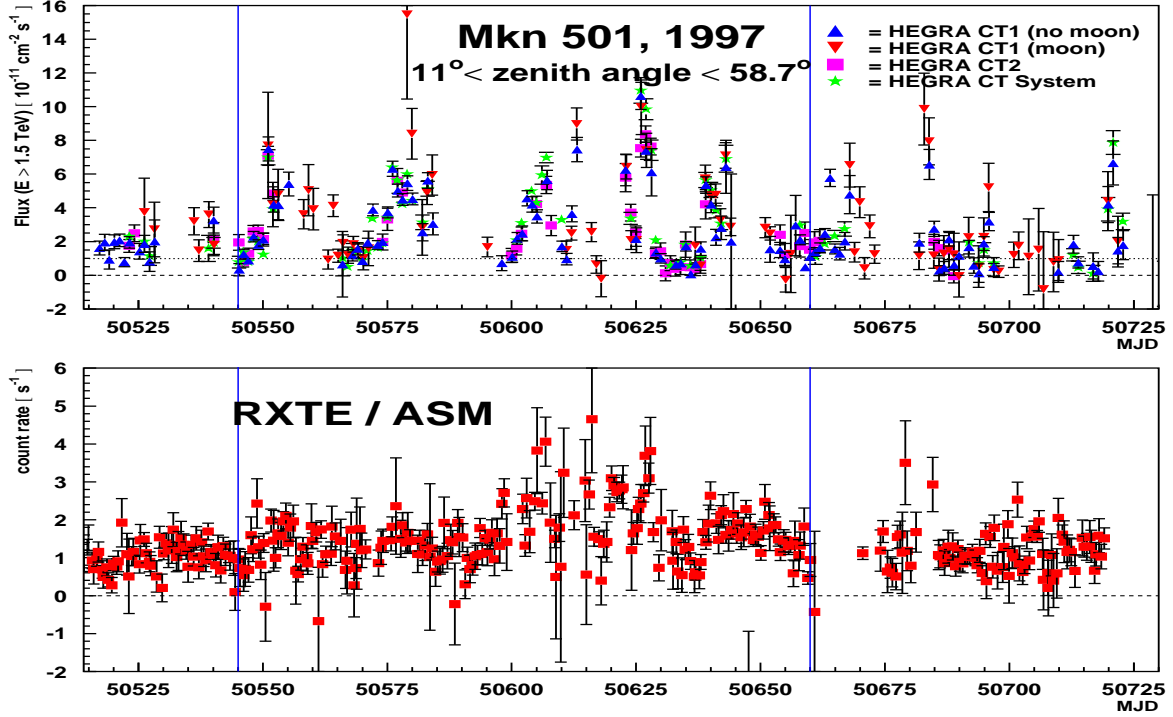


Fig. 1. TeV (upper) and X-ray (lower) lightcurve for Mkn 501 in 1997. The RXTE data was binned for visual purposes.

and the system response $f(t)$ represents the convolution of the response function $h(t)$ with the input data $x(t)$:

$$\begin{aligned} f(t) &= h(t) * x(t) := \int x(\tau) h(t - \tau) d\tau \\ &= \sum_{i=1}^K a_i \cdot h(t - \tau_i) \end{aligned} \quad (2)$$

- $h(t)$ - response function to δ -type shots at time 0
- τ_i - time of i -th flare/shot
- a_i - Amplitude of i -th flare/shot
(replace a_i by $(a_i - \bar{a})$ in case $\bar{a} \neq 0$)
- K - denotes the number of independent flares/shots which contribute to the observed data

Due to the Convolution theorem, the Fourier transform $F(\omega)$ of the system response $f(t)$ is given by:

$$F(\omega) = \int_{-\infty}^{\infty} f(t) \exp(i\omega t) dt = H(\omega) X(\omega) \quad (3)$$

with $H(\omega)$ and $X(\omega)$ being the Fourier transforms of $h(t)$ and $x(t)$ respectively. The Fourier power of the shot noise model then becomes

$$|FF^*| = |H(\omega)|^2 \cdot |X(\omega)|^2 \quad \text{with} \quad (4)$$

$$|X(\omega)|^2 = \left(\sum_{i=1}^K a_i \cos(\omega\tau_i) \right)^2 + \left(\sum_{i=1}^K a_i \sin(\omega\tau_i) \right)^2. \quad (5)$$

Since a_i , τ_i and therefore $a_i \cos(\omega\tau_i)$ and $a_i \sin(\omega\tau_i)$ are randomly distributed, the two sums in eq. 5 are approximately normally distributed according to the central limit theorem. The mean of each sum is zero (by definition of the amplitudes a_i) and the variance is $\sigma_a^2 = 0.5K\bar{a}^2$. Therefore

$$|FF^*| = K\bar{a}^2 |H(\omega)|^2 \cdot \frac{|X(\omega)|^2}{2\sigma_a^2} \quad (6)$$

is χ^2 -distributed with 2 degrees of freedom and has a mean and variance equal to $K\bar{a}^2 |H(\omega)|^2$. This means that the probability distribution for $|FF^*|$ in the shot noise model is the exponential distribution, **independent of the flare shape** (i.e. exponential type flares, Gaussian type flares, etc.). The mean and variance of the mean Fourier power is frequency dependent.

For Gaussian type flares we have $|H(\omega)|^2 \propto \exp(-\omega^2\sigma^2)$ and the mean Fourier power of the shot noise model becomes:

$$\langle |FF^*| \rangle = A \cdot \exp(-\omega^2\sigma^2) \quad (7)$$

If we have a source power spectrum $P_X(\omega)$ which is mainly due to randomly distributed flares (i.e. only one or a few 'disturbed' frequencies, where an additional effect may show up), the 'undisturbed' frequencies can be used to estimate the shot noise parameters (A and σ of eq. 7). This is done with a maximum likelihood (ML) fit. Once the mean Fourier power is known, the renormalized Fourier power $P_X(\omega) / |FF^*|$ is χ^2 -distributed with 2 degrees of freedom and has a mean

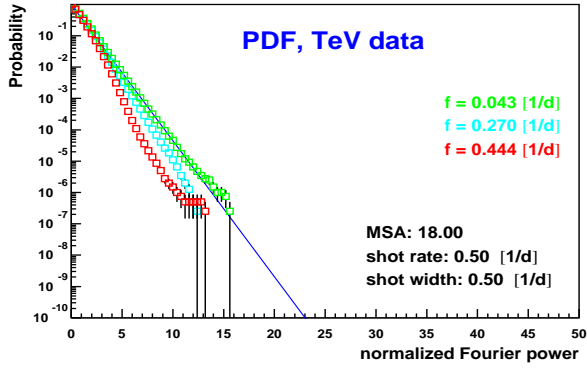


Fig. 2. PDF of the normalized Fourier power in the shot noise model for 3 different frequencies (the data spacing of the TeV data was used for the simulations). The simulation parameters: mean squared amplitude (MSA) of the flares, the flare rate and the flare width were chosen to match the values of the real data. The line denotes the expected exponential probability distribution.

and variance equal to unity. The ‘disturbed’ frequencies, of course, show deviations from this distribution.

The results from MC simulations (see next section) on the probability density function (*PDF*) of the shot noise model is shown in fig. 2. As can be seen, the PDF is very close to the exponential distribution for small frequencies. At the moon period and for larger frequencies, some larger deviations occur. These deviations are caused by the uneven data spacing. Since the derived PDF is always below the exponential probability distribution, the latter can be used for save probability estimations.

4 Estimation of shot noise parameters by the LS method

The unevenly sampled TeV and X-ray data have been analyzed using the formalism developed by Lomb and Scargle (Lomb 1976, Scargle 1982). In order to test the ability of the LS method to estimate the shot noise parameters A and σ , a series of MC simulations have been carried out (for details see Kranich 2001). The basic assumption of all simulations was an exponential distribution of the shot amplitudes a as well as for the time τ between consecutive shots:

$$pdf(a) = \frac{1}{\bar{a}} \cdot \exp(-a/\bar{a}); \quad pdf(\tau) = \lambda \cdot \exp(-\lambda\tau) \quad (8)$$

(λ denotes the shot rate). Each lightcurve was then built up of a superposition of Gaussian shaped flares with shot width σ (at the observation times t_i , which were taken from the real data). The simulated lightcurves were then analyzed with the LS method and the shot noise parameters A and σ were estimated with a ML fit. In order to cope with the uneven data spacing eq. 7 has been slightly modified for the LS power:

$$\langle P_X(\omega) \rangle = A \cdot \exp(-\omega^2 \sigma^2) + C \quad (9)$$

The constant C depends on the data spacing and the noise content and was estimated separately as $C = 2.20 \pm 0.45$ for the X-ray and $C = 0.43 \pm 0.10$ for the TeV data.

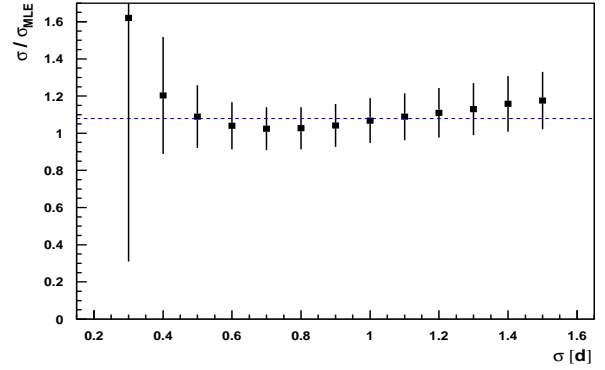


Fig. 3. Comparison between the shot noise parameter σ and the ML estimates σ_{MLE} for different shot widths σ . The errors were derived from the errors on the ML estimates. The line denotes the weighted mean.

The results of an ML fit of eq. 9 to the mean Fourier power spectrum, derived from 10000 individual simulations is shown in fig. 3. As can be seen, the resulting shot width σ_{MLE} is quite accurate for $\sigma > 0.4$ d. The results for the parameter A are not presented here, since this parameter has no clear physical meaning (it is mainly related to the signal to noise ratio in the corresponding lightcurve). For details the reader is referred to (Kranich 2001).

5 Independence of TeV and X-ray power spectra

In (Kranich, 1999) the final probability for the 23-day period was derived by combining the results from the X-ray and TeV power spectra (fig. 4 a and b and fig. 5). However, since the TeV and X-ray lightcurves are strongly correlated, one would expect to see the correlation also in the derived power spectra. This is not the case. Since the two data samples are very different (X-ray: 1894 data points, uniform spacing; TeV: 1999 data points, moon gaps, no observation during day time) the large fluctuations on the Fourier power spectrum (variance equal to the mean) lead to uncorrelated power spectra. Even when two data sets (one with the TeV spacing and one with the X-ray spacing) were taken from the same simulated set of flares the mean correlation was weak ($corr(\gamma, X-ray) = 0.33 \pm 0.24$ compared to $corr(\gamma, X-ray) = 0.0 \pm 0.22$ for two independent flare samples (The calculation of all the correlation coefficients was restricted to small frequencies $f < 0.2 \text{ d}^{-1}$ since this is the important region concerning the 23-day periodicity). In reality TeV and X-ray samples belong to different populations (e.g. synchrotron photons vs. inverse Compton scattered photons) and the correlation is expected to be even smaller. Systematic effects in the determination of the flux values/count rates of the two data samples were not considered.

In case the correlation is calculated for the real power spectrum, it is strong if the 23-day period is included, but oth-

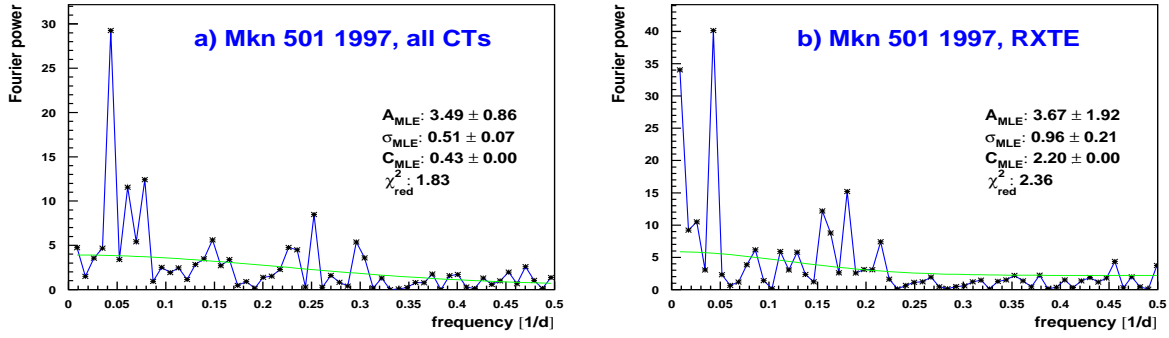


Fig. 4. The power spectra of the TeV (a) and X-ray (b) data sample and the corresponding mean Fourier power (green line). The 5th frequency, corresponding to the 23-day period was not included in the χ^2 calculation.

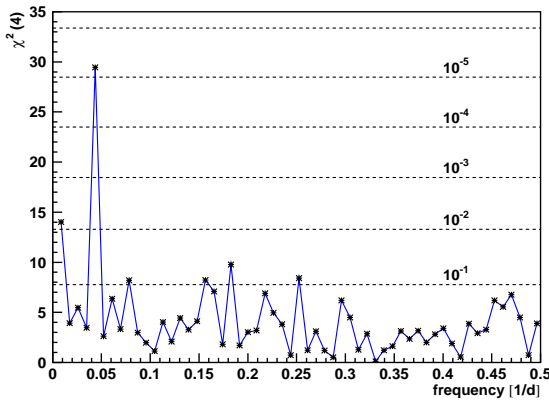


Fig. 5. The combined normalized power spectrum for the X-ray and TeV data. The dotted lines mark some probability levels.

erwise not present (e.g. $corr(\gamma, X - ray) = -0.01$. vs. $corr(\gamma, X - ray) = 0.57$ for included 23-day period).

If, on the other hand, the X-ray and TeV power spectra are correlated, then one would expect to see a deviation from the $\chi^2(4)$ -distribution in the data points of fig. 5. This effect can be investigated by transferring the $\chi^2(4)$ -distributed data points into $\chi^2(1)$ -distributed numbers. If the two power spectra have no significant correlation, the mean of the $\chi^2(1)$ -distributed numbers should be consistent with unity and significantly different otherwise. Again, the small frequency range $f < 0.2 \text{ d}^{-1}$ was used for this analysis and the 23-day period was excluded. The derived mean value was $\mu_{\chi^2(1)} = 1.04$ with a standard deviation of $\sigma_{\chi^2(1)} = 1.17$. Given the $N = 20$ test frequencies, the error on the mean becomes $\sigma(\mu_{\chi^2(1)}) = \sigma_{\chi^2(1)}/\sqrt{N} = 0.262$ and the deviation of the derived mean from unity is $(\mu_{\chi^2(1)} - 1)/\sigma(\mu_{\chi^2(1)}) = 0.15$ standard deviations. Thus the combined TeV and X-ray probabilities are basically uncorrelated when excluding the 23-day period and jointly behave as Gaussian white noise.

6 Results

Using the reanalyzed CT1 data, the probability for the 23 day period becomes $\mathcal{P} = 6.3 \cdot 10^{-6}$ corresponding to 4.4σ , which reduces to $\mathcal{P} = 3.6 \cdot 10^{-4}$ or 3.4σ after taking all 57 independent trial frequencies into account.

Deviations from this result may be obtained if different flare types, i.e. exponential type flares, are used in the shot noise model (this will change eq. 7 and 9). Furthermore, it could be argued that the prominent frequency components (e.g. the 23-day period) should be removed from the power spectrum before the ML fit is carried out. In the case of uneven data spacing, these prominent modes affect the whole power spectrum and therefore the ML fit (see Kranich 2001 for details). If these effects are used to estimate an error on the significance, the significance becomes $3.4^{+0.7}_{-0.5}\sigma$ or $3.4^{+1.1}_{-1.0}\sigma$ when the error on the ML estimate A is used ($A_{\gamma} = 3.49^{+1.0}_{-0.75}$ and $A_{X-ray} = 3.67^{+2.44}_{-1.56}$). The error on the 23-day period can be derived from the FWHM of the Fourier power peaks (using oversampling) as: $p_{X-ray} = 23.0^{+1.8}_{-2.0} \text{ d}$ and $p_{\gamma} = 22.5^{+1.8}_{-1.7} \text{ d}$ for the X-ray and TeV range respectively.

In case the 23-day period is related to some intrinsic properties of Mkn 501, it should show up in the next high state of the object. It should also be possible to give the final answer concerning the 23-day periodicity then.

Acknowledgements. The support of the HEGRA experiment by the BMBF (Germany) and the CYCIT (Spain) is acknowledged. We are grateful to the Instituto de Astrofísica de Canarias for providing excellent working conditions on La Palma.

References

- de Jager, O.C., et al., 26 ICRC (Salt Lake City), 3, 346, 1999
- Kranich, D., et al., 26 ICRC (Salt Lake City), 3, 358, 1999
- Kranich, D., et al., 1999, Aph 12, 65
- Kranich, D., PhD thesis, 2001, Technische Universität München
- Lomb, N.R., 1976, ApSS, 39, 447-462
- Protheroe, R.J., et al., 1997, Proc. 25th ICRC, Durban, Vol. 8, 317
- Remillard, R.A. & Levine, M.L., 1997, Proc. All Sky X-Ray Observations in the Next Decade
- Scargle, J.D., 1982, ApJ 263, 835